Chinese Chemical Letters 35 (2024) 109598

Contents lists available at ScienceDirect

Chinese Chemical Letters

journal homepage: www.elsevier.com/locate/cclet

Carbon dots-based dopamine sensors: Recent advances and challenges

Chenghao Liu[a], Xiaofeng Lin[a,*], Jing Liao[a], Min Yang[a], Min Jiang[a], Yue Huang[a], Zhizhi Du[a], Lina Chen[a], Sanjun Fan[b,*], Qitong Huang[a,*]

[a] Key Laboratory of Prevention and Treatment of Cardiovascular and Cerebrovascular Diseases of Ministry of Education, Key Laboratory of Biomaterials and Biofabrication in Tissue Engineering of Jiangxi Province, Key Laboratory of Biomedical Sensors of Ganzhou, School of Medical and Information Engineering, School of Pharmacy, Scientific Research Center, Gannan Medical University, Ganzhou 341000, China
[b] Department of Chemistry and Biochemistry, The Ohio State University, Columbus, OH 43210, United States

ARTICLE INFO

Article history:
Received 9 December 2023
Revised 26 January 2024
Accepted 29 January 2024
Available online 4 February 2024

Keywords:
Dopamine
Carbon dots
Fluorescent sensors
Colorimetric sensors
Electrochemical sensors

ABSTRACT

Dopamine, a pivotal excitatory neurotransmitter, plays a crucial role in metabolic, cardiovascular, renal, central nervous, and endocrine systems. Abnormal dopamine within the human body can cause various diseases. Therefore, the precise quantification of dopamine levels, both *in vivo* and *in vitro*, holds paramount significance for clinical applications and physiological investigations. Carbon dots (CDs) exhibit a plethora of remarkable properties, including a substantial specific surface area, robust electrical conductivity, commendable biocompatibility, minimal toxicity, and high photostability. Considering these unique characteristics, CDs demonstrate substantial potential for fluorescent sensors, colorimetric sensors, and electrochemical sensors for dopamine detection. This review systematically examined the challenges and prospects for the utilization of CDs-based fluorescent sensors, electrochemical biosensors, and colorimetric sensors for monitoring dopamine levels in recent years. These findings unveil promising avenues for further advancements in the field of dopamine detection.

1. Introduction

Dopamine, a crucial catecholamine neurotransmitter, intricately regulates metabolic processes, the central nervous system, cardiovascular functions, hormonal balance, and the renal system [1,2]. In both body fluids and brain tissues, dopamine exists as an organic cation that modulates various physiological functions, including memory persistence, physical movement, sleep, learning, social interaction, and cognitive skills [1–3]. Hence, significant deviations from normal dopamine concentrations within the body can result in a range of issues. High dopamine levels may contribute to conditions such as hypertension and heart failure [4], whereas low levels are implicated in conditions such as schizophrenia, Huntington's chorea, and Parkinson's disease [5,6]. Therefore, the development of a rapid, sensitive, and simple method for dopamine detection is crucial for physiological studies as well as for the diagnosis and treatment of related diseases. Currently, several analytical techniques have been employed for dopamine detection, such as colorimetric methods, electrochemical methods, capillary electrophoresis, fluorescence sensors, high-performance liquid chromatography, enzyme-linked immunosorbent assay (ELISA) [7–13]. Although the above methods have made certain contributions to the detection of dopamine, many researchers are continuously conducting related research to prepare more sensitive, accurate, and stable dopamine detection methods, hoping to achieve high sensitivity and stability in dopamine detection as soon as possible, and ultimately achieve commercialization.

In 2004, Xu *et al.* serendipitously discovered and reported the existence of fluorescent nanoparticles during the purification of single-walled carbon nanotubes through gel electrophoresis [14]. Subsequently, in 2006, Sun *et al.* employed laser ablation of "carbon targets" derived from graphite powder and cement, augmenting the photoluminescence of carbon nanoparticles *via* surface passivation with polyethylene glycol (PEG) [15]. This pioneering approach led to the nomenclature of the resultant carbon nanoparticles as "carbon dots (CDs)" for the first time. CDs are zero-dimensional carbon nanoparticles smaller than 10 nm with a passivated surface and intense fluorescence [16]. Typically, CDs exhibit amorphous or nanocrystalline nuclei that are predominantly composed of sp^2-hybridized carbon. CDs can be categorized into three principal types based on the nature of their carbon nuclei: graphene quantum dots (GQDs), carbon nanodots (CNDs), and carbon polymer dots (CPDs). GQDs derived from graphene and/or graphene oxide possess morphological characteristics that

* Corresponding authors.
E-mail addresses: Linxf@gmu.edu.cn (X. Lin), fan.1113@osu.edu (S. Fan), hqt@gmu.edu.cn (Q. Huang).

https://doi.org/10.1016/j.cclet.2024.109598
1001-8417/

mimic both CDs and graphene, affording GQDs with similar physical and chemical properties to graphene [17–19]. CNDs are surface-passivated carbon nanomaterials, typically less than 10 nm in size, displaying a discrete quasi-spherical morphology. Unlike GQDs, they are anisotropic with lateral dimensions exceeding their height [20]. CPDs are cross-linked products obtained through the dehydration condensation and carbonization of polymer precursors, featuring a "core-shell" nanostructure, where the carbon core and attached polymer chains (shells) self-assemble into CPDs [21]. Functioning as an amalgamation of semiconductor quantum dots and carbon materials, CDs combine the advantages of both. Compared to traditional semiconductor quantum dots and organic dyes, CDs exhibit superior photostability, including resistance to photodegradation, high bleaching resistance, and light scintillation, coupled with high photoluminescence quantum yields. Additionally, CDs have low toxicity, abundant precursor sources, and excellent biocompatibility [22–33]. These distinctive features have propelled intensive research on CDs across diverse domains, including sensing, bioimaging, drug loading, phototherapy, catalysis, and environmental applications [34–43]. In order to better detect dopamine, most of the CDs currently used contain carboxyl groups, which have good stability and can interact with amine groups in dopamine through electrostatic interactions. In addition, the π-π stacking between CDs and DA enhances electron transfer and communication, effectively constructing CDs-based dopamine sensors [9,10]. Therefore, more and more researchers are constructing various novel dopamine sensors through the interaction between CDs and dopamine. A comprehensive literature search was conducted on the "Web of Science" spanning from 2013 to 2023, utilizing the keywords "carbon dots", or "graphene quantum dots", or "carbon nanodots", or "carbon polymer dots" and "dopamine detection". The analysis revealed a steady rise in publications pertaining to the utilization of CDs for dopamine detection, particularly from 2015 onwards, underscoring the significant promise of CDs in dopamine detection (Fig. S1 in Supporting information). Furthermore, CDs are frequently used with other materials to formulate high-performance carbon-dot-based composites, enhancing the efficiency of dopamine detection for rapid, sensitive, and highly specific outcomes. This paper comprehensively reviews the applications of CDs in dopamine detection, focusing on three facets: electrochemical, fluorescent, and colorimetric sensors. In addition, the future directions and prospects of carbon-dot-based nanomaterials for diverse applications are discussed.

2. Carbon dots-based dopamine sensors

2.1. Fluorescent sensors

Fluorescence sensors offer advantages, such as operational simplicity, rapid detection, and high sensitivity [44–48], the fluorescent sensors demonstrate swift and precise measurements of dopamine at various concentrations [49,50], indicating elevated sensitivity and reproducibility. Notably, these sensors can detect dopamine at nanomolar levels, with a broad spectral range that minimizes interference from potential biomolecules [51]. Within the realm of fluorescent sensors, interaction with dopamine induces a change in fluorescence intensity, forming the basis for detection. CDs, which are renowned for their exceptional photostability, luminescence, and wide spectral absorption, have been incorporated into dopamine fluorescent sensors. In a study by Zhang *et al.* [52], CDs with yellow fluorescence were successfully synthesized from *Epimedium* using a green synthesis method. The dopamine detection mechanism involved quenching the CDs' fluorescence through electrostatic interaction with dopamine, resulting in an excellent sensor with a wide linear range of 0.1–1000 μmol/L and a low limit of detection (LOD) of 0.087 μmol/L. The subsequent addition of hydrogen peroxide gradually restored fluorescence by disrupting electrostatic interactions (Fig. 1A). In a parallel effort, Lan *et al.* employed a hydrothermal method to synthesize CDs with a fluorescence quantum yield (QY) of 49% using 1,3,6-trinitropyrene and Na_2SO_3 as raw materials. These CDs served as fluorescent probes for the detection of iron ions and dopamine [53].

Enzymes are invaluable macromolecular catalysts because of their efficient catalytic capabilities and substrate specificity [54]. However, their application is hindered by issues such as poor stability, limited reusability, and high cost. Immobilization technology has addressed these limitations, facilitating broader enzyme applications [55]. Research has demonstrated that the immobilization of enzymes in nanomaterials not only fully exposes the enzyme's active site, but also preserves its inherent conformation [56]. Additionally, the exceptional properties of integrated nanomaterials remain intact. Tang *et al.* developed a conjugated carbon-dot-tyrosinase bio-fluorescent probe by covalently coupling tyrosinase to CDs (Fig. 1B) [57]. This probe inherited the optical properties of CDs and the specific and efficient catalytic properties of tyrosinase (TYR). The resulting sensor exhibited good photostability, excellent selectivity, and a high sensitivity to dopamine. Tyrosinase catalyzes the oxidation of dopamine to produce dopaquinone, which in turn induces the fluorescence of CDs through an electron transfer process. The sensor demonstrated a detection range of 0.1–6.0 μmol/L with a limit of detection of 60 nmol/L, and successfully detected dopamine levels in human serum.

Enhancing the fluorescence properties of CDs remains a formidable challenge, with various factors influencing their optical characteristics, including the synthesis method, precursors, passivation, and heteroatom doping [58]. Extensive investigations have been conducted to improve the photoluminescence (PL) properties of CDs, with a particular focus on improving their fluorescence quantum yield. Numerous methods have been proposed to enhance the photophysical characteristics of CDs, such as doping and surface passivation [59]. Notably, heteroatom doping has consistently exhibited a positive impact on both the QY and PL lifetime of CDs, emerging as a pivotal factor influencing their optical properties [60–63]. Therefore, doping is an effective strategy to modulate the photophysical attributes of CDs. Based on the number of doped heteroatoms, doping can be categorized as single doping and co-doping. Currently, synthetic methods for doped CDs include hydrothermal, pyrolysis, microwave-assisted, electrochemical treatment, and other methods [64–67].

Nitrogen, a prevalent dopant, is commonly used to enhance the PL of CDs. Given the similar atomic radii of nitrogen and carbon atoms, nitrogen doping has been demonstrated to elevate the PL of CDs, concurrently introducing new surface defects that expand their applicability. Wang *et al.* reported the synthesis of nitrogen-doped carbon quantum dots (N-CQDs) with bright blue fluorescence using a straightforward solid heat method, incorporating glycine and urea as carbon and nitrogen sources [68]. The resulting quantum dots exhibited a QY of 21.04%, along with stable optical properties and resistance to acidic and alkaline conditions. Notably, the fluorescence of the N-CQDs can be effectively quenched by dopamine, rendering them suitable for use as a dopamine fluorescent probe. The quenching mechanism was attributed to the aggregation of N-CQDs and electron transfer from the N-CQDs to dopaquinone under alkaline conditions (Fig. 1C). The fluorescent sensor demonstrated excellent linearity in the range of 0.25–100 μmol/L, with a sensitivity of 0.0972 μmol/L. Furthermore, the sensor exhibited successful application in determining dopamine levels in human and rat sera, yielding high recoveries ranging from 98.24% to 107.86%, indicating promising prospects for practical applications. In a parallel study, Ma *et al.* synthesized a series of doped GQDs using the hydrothermal method (Fig. S2A in Support-

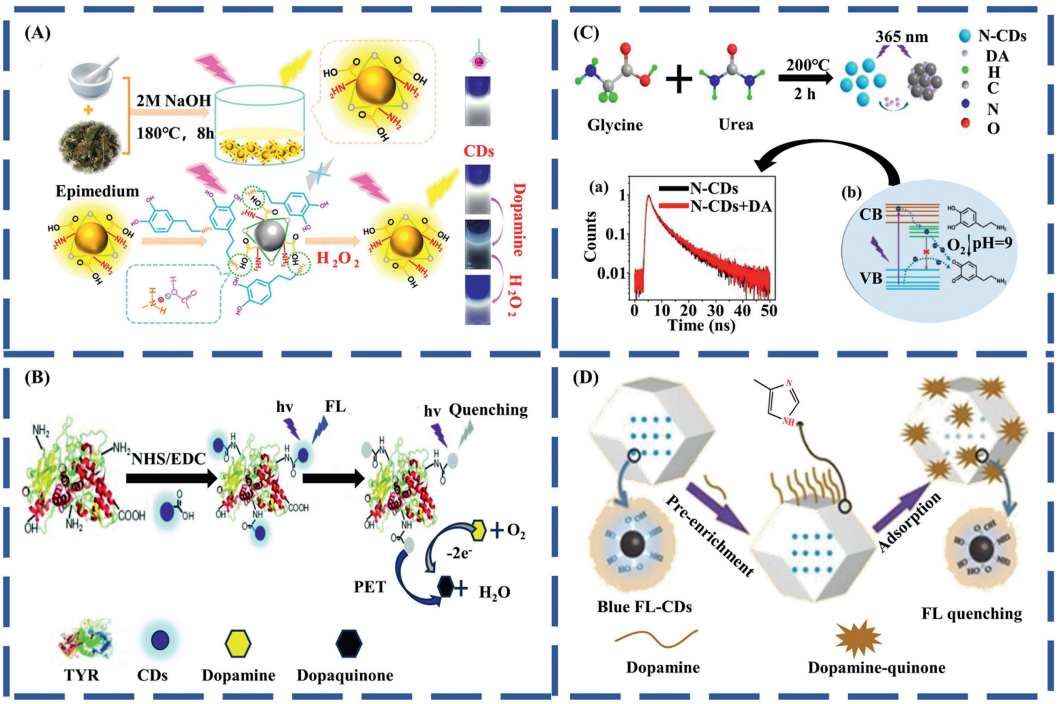

Fig. 1. (A) Synthesis scheme of CDs with Epimedium for dopamine and H_2O_2 detection. Copied with permission [52]. Copyright 2021, Elsevier. (B) Preparation and mechanism of CD-TYR biological probes for dopamine sensing. Reproduced with permission [57]. Copyright 2019, Royal Society of Chemistry. (C) Mechanism of dopamine in quenching the fluorescence of N-CQDs. (a) PL lifetime degradation of N-CQDs in the presence and absence of dopamine. (b) Schematic representation of electron transfer from N-CQDs to dopamine quinones. Copied with permission [68]. Copyright 2020, Elsevier. (D) The synthesis scheme of CDs@ZIF-8 and its application in dopamine sensors. Reproduced with permission [81]. Copyright 2020, Elsevier.

ing information). Elemental doping significantly augmented the QY of the GQDs, with N-doped GQDs utilizing citric acid (CA) as the C source and ethylenediamine as the nitrogen source, achieving the highest QY of 95% [69]. However, the N-GQDs did not exhibit fluorescence quenching in response to dopamine. Conversely, N-GQDs (QY = 78%) with urea as the N source were sensitive to dopamine-induced fluorescence quenching. Under optimal conditions, a strong linear correlation between fluorescence quenching efficiency and dopamine concentration was observed in the ranges of 10–3000 and 3000–7000 nmol/L, with corresponding LODs of 3.3 and 611 nmol/L, respectively. The quenching mechanism was attributed to the pyridine N structure of N-GQDs, expediting the selective sorption of the catechol group in dopamine molecules on the surface of N-GQDs and facilitating the formation of non-fluorescent complexes between N-GQDs and dopamine.

In contrast to single-heteroatom doping, co-doping with multiple heteroatoms has yielded remarkable improvements in the performance of CQDs owing to the synergistic effects between the doped heteroatoms. Wang *et al.* devised a novel fluorescent probe based on S, N-CQDs, which exhibited high selectivity and sensitivity for dopamine. The probe was successfully applied to detect dopamine in real serum samples, achieving recoveries ranging from 96.85% to 102.72% [70]. Mathivanan *et al.* reported the first synthesis of nitrogen-iron-doped CDs (N, Fe-CDs) with a QY of 49.52% through a single-step microwave ablation route using ferric chloride hexahydrate, CA, and ethylenediamine as precursors [71]. The N, Fe-CDs exhibited excellent dispersion and photostability in aqueous solutions. The fluorescence of N, Fe-CDs was progressively quenched with increasing dopamine concentrations within the range of 0.5–300 μmol/L, demonstrating a LOD of 0.07 μmol/L. Furthermore, N, Fe-CD-based fluorescent probes employing the internal filtering effect have been developed for 4-nitrophenol (4-NP) detection. The sensor exhibited exceptional performance in detecting dopamine and 4-NP in serum and water samples. Consequently, N- and Fe-CDs hold significant promise as sensors in diverse biological and environmental applications.

Functionalization is an effective strategy for enhancing the surface properties of CDs, potentially leading to elevated QY and other advantageous characteristics [72,73]. Mahmoud *et al.* successfully synthesized β-CD/N@GQDs through the functionalization of nitrogen-doped graphene quantum dots (N@GQDs) with β-cyclodextrin (β-CD) [74]. By leveraging β-CD/N@GQDs, they devised a dopamine fluorescence sensor and dopamine colorimetric sensor (Fig. S2B in Supporting information). In the colorimetric approach, β-CD/N@GQDs serve as catalysts, initiating the oxidation of tetramethylbenzidine (TMB) to blue-oxidized TMB (oxTMB) by H_2O_2. The subsequent addition of dopamine reduced oxTMB, thereby altering its color. In the dopamine fluorescent sensor, the fluorescence of β-CD/N@GQDs experienced quenching in the presence of oxTMB due to the "internal filtration effect". The introduction of dopamine restored fluorescence intensity by reducing oxTMBH to TMB. Under optimized conditions, the colorimetric sensor demonstrated a linear range of 0.12–7.5 μmol/L, with a LOD of 0.04 μmol/L [signal-to-noise ratio (S/N) = 3]. Simultaneously, the fluorescent sensor exhibited a linear range of 0.028–1.5 μmol/L, with an LOD of 0.009 μmol/L (S/N = 3). However, this sensor suffers from the inherent limitation that elevated concentrations of reducing compounds, such as glutathione and ascorbic acid, in biological fluids may interfere with dopamine detection.

Metal-organic frameworks (MOFs) represent a rapidly evolving class of hybrid porous materials formed through the self-assembly of metal nodes and organic ligands in recent years. MOFs are versatile platforms that offer precise control over the composition, pore shape and size, and surface chemical environment at the molecular scale [75,76]. Collaborative interactions between ligands and metals in MOFs enable the formation of diverse pore structures, substantial specific surface areas, and distinctive fluorescence properties. This synergy facilitates the straightforward

construction of luminescent platforms with adjustable luminescent properties and diverse detection mechanisms [77–80]. In a study by Xie *et al.* [81], luminescent metal-organic frameworks (LMOFs) were synthesized by incorporating CDs with high fluorescent quantum yield into zeolitic imidazolate frameworks-8 (ZIF-8). Utilizing the CDs@ZIF-8 composite, they developed a highly sensitive and selective fluorescent dopamine sensor for the intricate detection of dopamine in serum and urine (Fig. 1D). In this fluorescent sensor, ZIF-8 pores efficiently preconcentrated the target substance dopamine, independently oxidizing it to dopaquinone through the alkaline sites provided by ZIF-8. Dopaquinone was adsorbed onto the ZIF-8 framework *via* π-π interactions with the aromatic rings of ZIF-8. Additionally, electrostatic interactions between dopaquinone and the CDs lead to fluorescence quenching of the CDs. The synergistic interaction between the CDs and ZIF-8 further enhanced this process. The sensor exhibited good linearity with dopamine concentrations ranging of 0.1–200 μmol/L, with a low LOD of 16.64 nmol/L.

The fluorescence intensity of single-wavelength fluorescent probes is prone to influences, such as photovoltaic system drift, variations in probe concentration, and autofluorescence within intricate biological systems [82]. To address these limitations, the ratiometric fluorescent method is advantageous. This strategy involves quantifying the ratio of fluorescence emission intensities from two or more independent channels within the sensing system following the detection of the target analyte. Utilizing the signal from one of the channels as a reference allows for the correction and normalization of signals from other channels [83]. Sun *et al.* [84] devised a ratiometric fluorescent sensor based on a composite of CD-modified hydroxyapatite nanowire-lanthanide metal-organic frameworks (Fig. S2C in Supporting information). The construction employed a straightforward solvothermal method and a self-assembly technique. The sensor demonstrated notable benefits including high stability, strong selectivity, and rapid detection speed. Importantly, dopamine concentrations were successfully measured in serum.

As shown in Table S1 (Supporting information), the recent applications of fluorescent CDs and CDs-based nanocomposites in the detection of dopamine by using fluorescence sensors have been summarized in recent years [49,50,52,53,57,68-71,74,81,82,84-119]. Despite the many known advantages of fluorescence sensing, its practical application faces many challenges. Their fundamental properties and photoluminescence mechanisms, mechanisms need to be further explored. Furthermore, currently, the fluorescence sensors based on CDs for the detection of dopamine mainly emit light in the green and blue regions, which makes it impossible to directly detect dopamine *in vivo*. Therefore, the development of high-performance near-infrared CDs is expected to achieve real-time detection of dopamine *in vivo*.

2.2. Electrochemical sensors

Electrochemical sensors offer a range of advantages, including multiplex analysis, excellent selectivity, high sensitivity, low detection limits, rapid response, ease of miniaturization, cost-effectiveness, and straightforward operation [120–126]. Notably, they uniquely enable the analysis of living organisms [127,128]. Exploiting the favorable electrochemical response of dopamine, the hydroxyl group of its benzene ring undergoes oxidation to produce quinone under an electric current with subsequent reduction, facilitating electrochemical detection. However, the simultaneous presence of ascorbic acid (AA) and uric acid (UA) with dopamine poses challenges because of their similar oxidation potentials on bare electrodes [129,130]. Despite the speed and simplicity of electrochemical methods, their stability is insufficient. Therefore, over the past decades, researchers have extensively focused on enhancing electrode modification materials to achieve more accurate, and stable dopamine detection. CDs, which are characterized by high electrical conductivity, large specific surface area, low toxicity, and good biocompatibility [131], have emerged as crucial subjects in electrochemical sensor research. Wang *et al.* synthesized CDs using a one-step ultrasound technique with glucose as the carbon source [132]. The CDs were electrochemically deposited and immobilized on a glassy carbon electrode (GCE) to prepare CDs/GCE. Differential pulse voltammetry (DPV) was employed for simultaneous detection of dopamine, UA, tryptophan (Trp), and theophylline (TP). Electroluminescence (ECL), which combines chemiluminescence and electrochemistry [133], has garnered interest across various fields, such as biomarker analysis, environmental monitoring, and drug analysis, owing to its inherent advantages including simplicity, cost-effectiveness, high signal-to-noise ratio, high sensitivity, wide dynamic range, and rapid response [134,135]. Zhu *et al.* synthesized CDs with different fluorescence colors *via* a green hydrothermal method using glucose and potassium phosphate as raw materials. The particle size and fluorescence color of the CDs depended on the amount of potassium phosphate [136]. Yellow fluorescent CDs with robust photostability were used to construct a sensing platform for dopamine detection (Fig. 2A). The ECL intensity of the CDs exhibited an inverse correlation with dopamine concentration in the range of 0.01–100 μmol/L. Moreover, the dopamine detection process is unaffected by both AA and UA.

Among various nanomaterials, carbon-based nanomaterials exhibit considerable promise for electrode modification. Notably, carbon nanotubes (CNTs) and graphene are excellent and promising carbon-based nanomaterials owing to their distinctive structures and exceptional electrochemical properties. These carbon-based nanomaterials commonly possess advantageous features, including low cost, good biocompatibility, non-toxicity, large surface area, and high electrical conductivity [137–139]. Therefore, researchers have frequently combined CDs with other carbon-based nanomaterials to prepare nanocomposites with enhanced electrochemical properties through synergistic interactions. In a recent study, Huang *et al.* developed a novel, straightforward, and cost-effective electrochemical sensor by modifying a GCE with GQDs and multi-walled carbon nanotubes (MWCNTs) for the highly sensitive and selective detection of dopamine in AA and UA (Fig. 2B) [140]. The electron transfer of dopamine was facilitated by the large conjugated π-bonds in the GQDs-MWCNTs nanocomposite. In addition, GQDs with a considerable number of anionic groups exhibited the ability to attract cations, thereby enhancing the sensor selectivity. Using DPV, the GQDs-MWCNTs/GCE sensor demonstrated exceptional sensitivity for dopamine, with a robust linear range of 0.005–100.0 μmol/L and a LOD of 0.87 nmol/L. Notably, this sensor was successfully applied for the first time to detect dopamine release from live PC12 cells.

Pan *et al.* synthesized a porous organic polymer (POP) through Friedel-Crafts alkylation, followed by direct carbonization of POP at 800 °C under argon gas to yield porous carbon [141]. The obtained porous carbon served as a carbon source for controlling the composition of the GQDs through nitric acid oxidation (Fig. 2C). An ECL sensor was developed using a GQD/chitosan-graphene composite-modified GCE for dopamine detection. Remarkably, the sensor exhibited ultra-high selectivity for dopamine, even in the presence of interfering substances at a concentration ratio of 100. Furthermore, the sensor was successfully employed for the detection and quantification of actual dopamine in human samples.

Metals such as gold, silver, copper, and their oxides have been widely explored in electrochemistry owing to their signal detection and amplification capabilities. In particular, Ag NPs have garnered attention as catalysts because of their excellent electron transfer and catalytic properties for various chemical reactions.

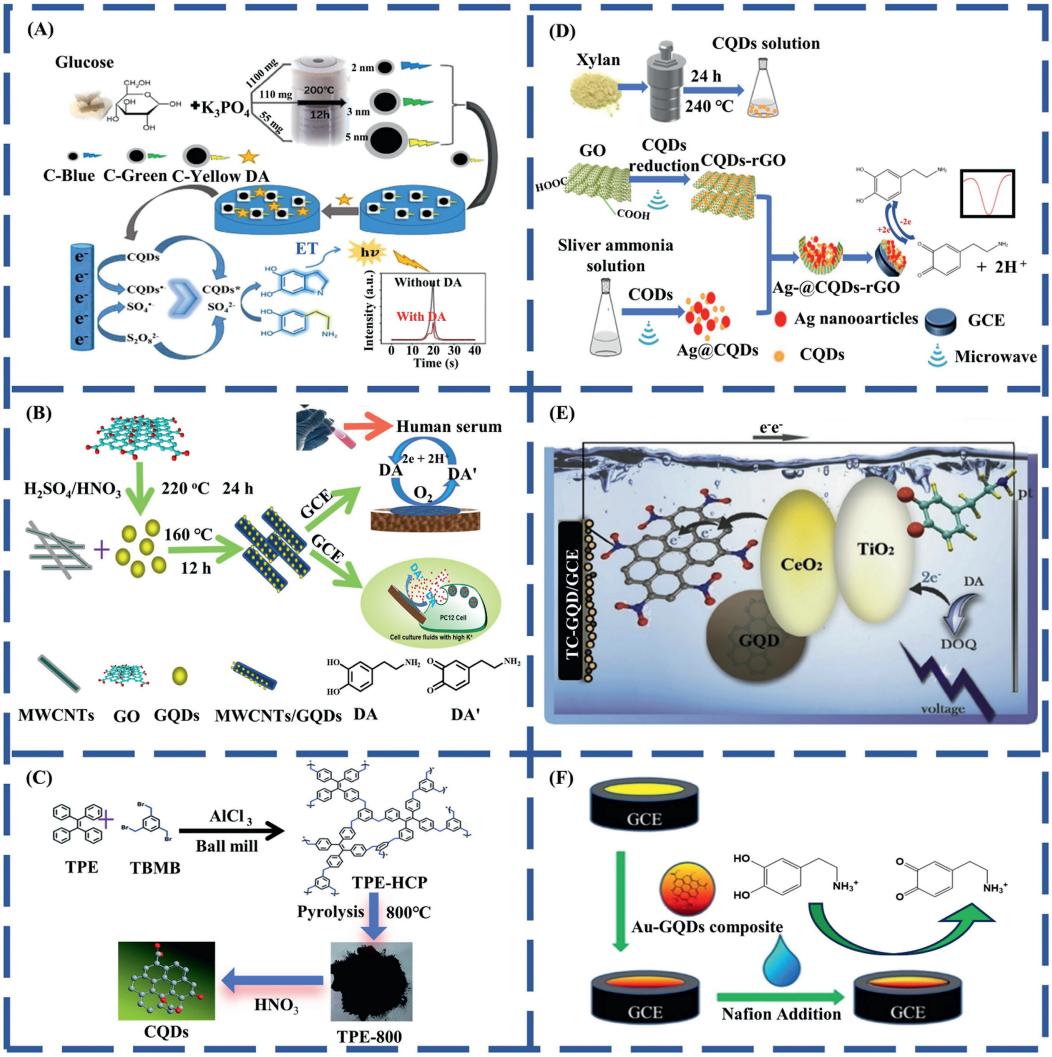

Fig. 2. (A)Schematic diagram of the ECL sensor for the detection of dopamine. Reproduced with permission [136]. Copyright 2022, Elsevier. (B) Schematic diagram of the MWCNTs/GQDs-based electrochemical dopamine sensor. Reproduced with permission [140]. Copyright 2020, American Chemical Society. (C) Typical preparation routes of TPE-HCP and corresponding porous carbon (TPE-800) and synthesis of CQDs. Reproduced with permission [141]. Copyright 2019, Royal Society of Chemistry. (D) Schematic diagram of Ag@CQDs-rGO/GCE for dopamine detection. Reproduced with permission [143]. Copyright 2020, Elsevier. (E) Mechanistic diagram of EC electron transfer in TC-GQD/GCE in the presence of dopamine. Reproduced with permission [146]. Copyright 2019, Elsevier. (F) Diagram of Au-GQDs-Nafion/GCE preparation and the voltammetric measurement of dopamine. Reproduced with permission [155]. Copyright 2019, Elsevier.

Incorporating Ag NPs onto electrodes enhances electron transfer between the electrode and the active substrate, as well as between analyte molecules and the substrate [142]. Despite their utility, the reducing agents traditionally used in Ag NPs synthesis are often expensive and toxic. To address this, Han *et al.* synthesized Ag NPs and reduced graphene oxide (rGO) using xylan-based carbon quantum dots as reducing agents and stabilizers [143]. They modified a glassy GCE with an Ag@CQDs-rGO nanocomposite to establish highly sensitive sensors for dopamine detection (Fig. 2D). Based on the electrochemical impedance spectra recorded for various modified GCEs in a 0.1 mol/L phosphate buffer saline (PBS) solution containing 200 μmol/L dopamine at an open-circuit potential, the impedance of the Ag@CQDs-rGO/GCE is lower than that of other modified electrodes. This result can be attributed to the enhanced conductivity of Ag NPs, imparting higher sensitivity to dopamine to the Ag@CQDs-rGO-modified GCE. The CQDs in this sensor contribute not only to the improved electrode conductivity but also to the heightened selectivity for dopamine, achieved through electrostatic interactions between the amine functional group and the carboxyl group. Hence, the developed sensor exhibits the capability to detect dopamine over a broad linear range (0.1–300 μmol/L) with a low detection limit of 1.59 nmol/L. Furthermore, the sensor demonstrates successful application in detecting dopamine in dopamine injection and bovine serum solution samples

Titanium dioxide (TiO_2) is recognized as a wide-gap semiconductor within the realm of metal oxides because of its cost-effectiveness, robust photocatalytic activity, commendable electrical conductivity, physical and chemical stability, biocompatibility, non-toxicity, abundance, and resilience to photochemical degradation [144,145]. Ahmadi *et al.* employed a hydrothermal method to synthesize a titanium-cerium-graphene quantum dot (TC-GQD) nanocomposite for the development of electrochemical and photoelectrochemical sensors for dopamine detection [146]. Through analysis using diffuse reflectance spectroscopy (DRS) and an electric conductivity meter, the study revealed a shift in the bandgap of the TC-GQD nanocomposite to visible light (1.3 eV) for its constituents. This phenomenon indicates that the cerium doping in TiO_2 has a pronounced effect on TiO_2. Furthermore, the conductivity increased significantly to 89.5 μS/cm, demonstrating the enhanced conductivity of the material owing to the synergistic ef-

fect between the components in the TC-GQD nanocomposite. In a 0.1 mol/L PBS solution containing 1 mmol/L AA, 100 μmol/L UA, and different concentrations of dopamine (0, 5, 25, and 100 μmol/L), DPV was employed to investigate the electrochemical behavior of single-component modified electrodes and a nanocomposite-modified electrode. The results revealed that only TC-GQD/GCE exhibited three distinct peaks corresponding to AA, dopamine, and UA at 180, 400, and 580 mV, respectively (Fig. 2E). The unique structure of TiO_2 facilitated efficient electron transfer within the nanocomposite. Meanwhile, the high conductivity of the nanocomposite not only accelerated electron transfer but also enhanced the oxidation tendency of dopamine.

Polymer film-modified electrodes offer notable advantages, including excellent selectivity, stability, reproducibility, excellent electrical conductivity, and consistent chemical performance [147–149]. Within the realm of conductive polymers, polyaniline has garnered significant attention owing to its facile synthesis, environmental stability, cost-effectiveness, controlled conductivity, remarkable electrical properties, chemical stability, and compatibility with other substances [150–152]. By leveraging these attributes, Ratlam *et al.* employed electrostatic spinning to prepare electrospun nanofiber films of PANi/CQDs, utilizing them in the construction of dopamine electrochemical sensors [92]. Comparative tests demonstrated that under identical conditions, the current response signal of the PANi/CQD films exceeded that of the PANi films, attributed to the PANi/CQD composite surface being rich in functional groups such as hydroxyl, carboxyl, and amine groups. These groups facilitate interactions with dopamine molecules through π-π stacking and hydrogen bonding interactions. The CV results revealed a linear range for dopamine detection, from 10 μmol/L to 90 μmol/L, with an LOD of 0.1013 μmol/L. Furthermore, the PANi/CQD composite solution was used as a fluorescent sensor for dopamine detection.

Nafion membranes, recognized as perfluorosulfonic acid proton exchange membranes, are exemplary cation exchange membranes with superior ion exchange and electrochemical, chemical, and mechanical properties [153,154]. In a study by Jang *et al.* [155], Au-GQD composites were synthesized through a one-pot reaction, leading to the development of an Au-GQD-Nafion/GCE electrochemical sensor (Fig. 2F). The electrochemical behaviors of various electrodes were investigated in a 0.1 mol/L PBS solution (pH 7.4) using cyclic voltammetry (CV). Comparative analysis revealed that Au-GQD-Nafion/GCE exhibited a higher oxidation peak current than GQDs/GCE, AuNP/GCE, and Au-GQDs/GCE. This enhanced performance is attributed to the synergistic effect among the three materials. First, AuNPs enhanced the composite conductivity, facilitating electron transfer between the electrode and active matrix. Second, functional groups such as carboxyl groups in CQDs interacted with dopamine molecules through π-π stacking and hydrogen bonding, enhancing sensor sensitivity and selectivity. Finally, Nafion contributed to the stabilization of the Au-GQD composite. The cation transfer channels in the Nafion membrane facilitated the diffusion of dopamine molecules while counteracting neutral molecules and anions, significantly reducing the system response time.

As shown in Table S2 (Supporting information), the different types of CDs used in electrochemical sensors for the detection of dopamine have been summarized in recent years [92,108,132,136,140-143,146,155-182]. Electrochemical sensors have the advantages of multiplexed analysis, good selectivity, high sensitivity, low detection limit, fast response, easy miniaturization, low cost, simplicity, and ease of operation. However, the application of CDs in electrochemical sensors still faces challenges: (1) How to develop a more gentle, environmentally friendly, and novel preparation method to create CDs with better electrochemical performance? (2) How to design electrochemical sensors with excellent catalytic performance or activity toward dopamine? (3) How to miniaturize carbon-dot electrochemical sensors for *in-situ* detection?

2.3. Colorimetric sensors

The colorimetric method, which requires no sophisticated equipment but relies on the direct visual observation of color changes coupled with instruments such as ultraviolet–visible spectroscopy (UV–vis) spectrophotometers, fluorescence spectrometers, or color processing software to determine the concentration of the relevant components, offers economic and rapid advantages [183–186]. The integration of fluorometric and colorimetric sensors presents an avenue for enhancing the accuracy of dopamine detection. Li *et al.* introduced a dual-mode sensor, employing gadolinium(III)-doped CDs, for the straightforward, sensitive, and selective determination of dopamine hydrochloride (DH) and D-glutamic acid (D-Glu) (Fig. 3A) [112]. Gd-CDs with blue fluorescence were synthesized *via* a one-pot solvothermal method using polyetherimide and $GdCl_3$ as the precursors. Sensor selectivity was evaluated by comparing the fluorescence responses of Gd-CDs to different metal cations, DH, Glu, and other amino acids, demonstrating the high sensitivity and selectivity of Gd-CDs towards DH. At 465 nm, the fluorescence intensity of the Gd-CDs exhibited gradual quenching with increasing DH concentration, displaying excellent linearity within the 0–15 μmol/L range. This quenching resulted from complex formation between DH and Gd-CDs through electrostatic and coordination interactions. DH was concurrently detected by the UV–vis method in the 1–15 μmol/L range, accompanied by a visual color change from light white to dark yellow. In the Gd-CDs-DH system, competition between D-Glu and DH results in the formation of a more stable complex. This complex formation reduced the overall energy of the system, facilitating the $\pi \rightarrow \pi^*$ and $n \rightarrow \pi^*$ electron transitions. Consequently, the UV–vis absorption peaks exhibited a redshift, leading to the restoration of the Gd-CD fluorescence. This dual-mode sensor effectively detected DH and D-Glu in aqueous solutions, mouse serum, and human urine. Jia *et al.* synthesized CDs using glutathione, L-histidine, and formamide *via* a solvothermal method. These CDs were used to construct a novel colorimetric sensor for dopamine determination (Fig. 3B) [187]. Under illumination, the CDs generated singlet oxygen (1O2) from the dissolved oxygen, inducing a color change by oxidizing TMB. In the presence of dopamine, the catalytic activity of the CDs was inhibited, weakening the TMB complex absorption at 652 nm. Over a dopamine concentration range of 0.5–15 μmol/L, the color change exhibited a linear relationship, enabling the development of a dopamine colorimetric sensor based on CDs. This sensor demonstrated an impressive detection limit of 0.25 μmol/L and exhibited excellent selectivity and stability.

Smartphones have been seamlessly integrated with colorimetric sensors for applications in biochemical testing, environmental monitoring, and food surveillance owing to their inherent portability and capabilities for real-time monitoring [188–192]. The smartphone's built-in camera and dedicated applications serve as an analyzer or controller, enabling real-time, instantaneous, and remote transmission monitoring. This integration enhances system portability and reduces overall manufacturing costs. Crucially, smartphone-based detection systems mitigate individual variations in color recognition, thereby improving the detection accuracy. Chellasamy *et al.* pioneered a smartphone-integrated, additive-free, non-functionalized CQD-based fluorescent and colorimetric dopamine sensor (Fig. 3C) [107]. The fluorescent sensor demonstrated effective LOD values of 6, 8.5, and 8 nmol/L for deionized water, elderly male plasma, and elderly female plasma, respectively, within the linear range of 100 nmol/L to 1000 μmol/L. In the colorimetric mode, H-CQDs interacted with dopamine to

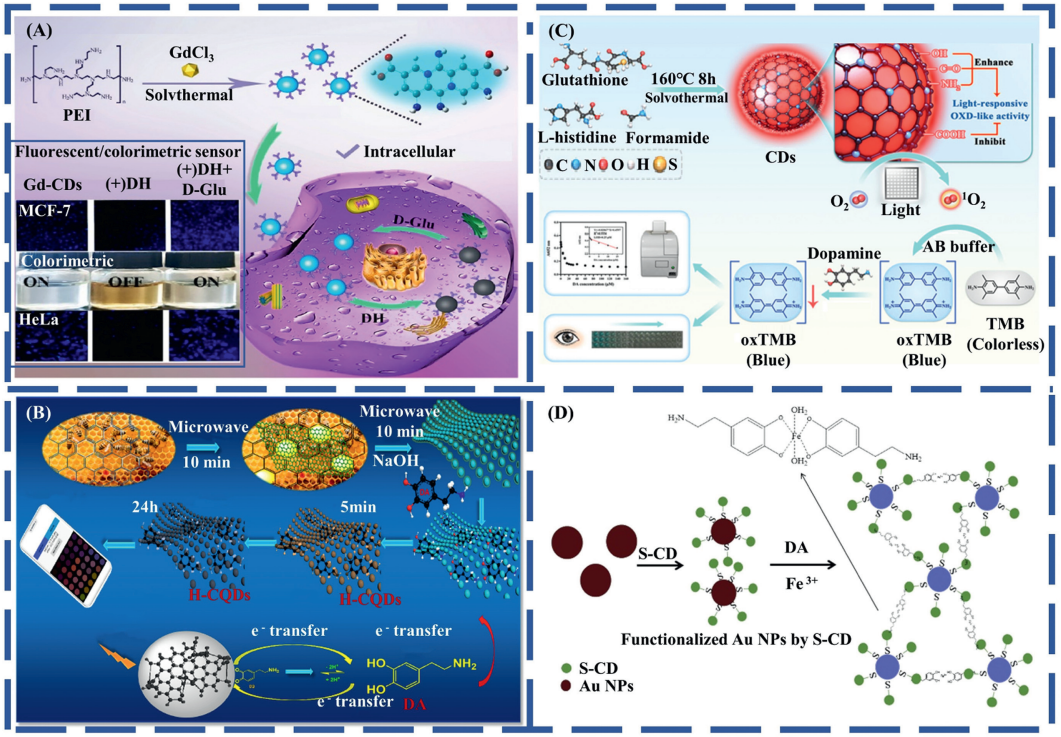

Fig. 3. (A) Gd-CDs as fluorescent and colorimetric dual-mode sensors for DH and D-Glu sensing and multi-type cell imaging. Reproduced with permission [112]. Copyright 2022, Elsevier. (B) Synthesis of CDs using glutathione, L-histidine, and formamide as precursors *via* the solvothermal method, enabling the construction of a novel colorimetric sensor for dopamine determination. Reproduced with permission [187]. Copyright 2023, Frontiers Media S.A. (C) Schematic diagram of the synthesis and operation of a smartphone integrated sensor. Reproduced with permission [107]. Copyright 2021, Elsevier. (D) Schematic diagram of S-CDs functionalized Au NPs aggregated by dopamine in the presence of Fe^{3+} ions. Reproduced with permission [197]. Copyright 2019, Elsevier.

form dopaquinone, inducing a color change in the H-CQD solution. Different concentrations of mixed solutions were added to the sensor array system and the array was imaged using a color array analysis application. The acquired images were processed using the application to effectively analyze the change in the sample color. In addition, quantification using UV–vis spectroscopy is feasible.

Typical metallic NPs, such as AuNPs, AgNPs, and CuNPs, exhibit localized surface plasmon resonance (LSPR). The agglomeration of metallic NPs induces a red shift in the SPR peak, resulting in observable color changes in the metallic nanoparticle solution to human eyes [183]. With this principle, numerous efficient colorimetric sensors have been devised [193–196]. A recent development involves the utilization of S-doped carbon-dot-functionalized Au NPs for dopamine detection (Fig. 3D) [197]. The carboxyl groups on the surface of S-CDs@AuNPs interacted with the amino groups of dopamine. Upon introduction of the linker Fe^{3+}, the dopamine-S-CDs@AuNPs aggregated, causing a red shift in the SPR peak of S-CDs@AuNPs from 520 nm to 670 nm. The signal for dopamine determination was derived from the absorption intensity ratio at 670 nm to 520 nm. Factors such as reaction time, solution pH, Au NPs concentration, and Fe^{3+} concentration were optimized. The colorimetric sensor exhibited excellent linearity for dopamine within the range of 0.81–16.80 μmol/L under optimal conditions. The sensor accurately detected dopamine in human urine and serum samples.

Previously reported on the CDs-based colorimetric assays for the detection of dopamine can be referred to in Table S3 (Supporting information) [74,99,106,107,121,197-199]. Despite the simplicity of the process of dopamine detection by colorimetric methods, CDs are less used in the detection of dopamine by colorimetric sensors. We should devise simple methods to synthesize multicolored CDs for visual detection of dopamine. An experimental protocol for the indirect detection of dopamine was designed to enhance the catalytic performance of CDs for dopamine, and the luminescence mechanism of CDs in this over was further investigated. Due to the occurrence of non-directional aggregation of CDs in solution, an unstable solution with large particle size and reduced surface repulsion is formed. This leads to imprecise target determination and reduces the detection sensitivity and stability. To achieve effective detection, background interference is minimized as much as possible during the assay.

3. Conclusion and future prospects

Dopamine is a crucial neurotransmitter that plays a pivotal role in human physiology. Deviation from normal dopamine concentrations in the body may lead to the onset of specific diseases. Accurate detection of dopamine concentration is crucial for disease prevention and diagnosis. However, traditional methods, such as high-performance liquid chromatography and ELISA, suffer from drawbacks such as prolonged analysis time, high labor intensity, and elevated costs. As a result, there is a pressing need for a new, rapid, and economical detection method with high sensitivity and selectivity. Electrochemical biosensors, which are known for their advantages in sensitivity, selectivity, and cost-effectiveness, are widely employed. Colorimetric and fluorescence methods are prominent for dopamine detection because of their simplicity, intuitiveness, ease of operation, rapidity, and high sensitivity. The choice of electrode materials for electrochemical sensors and fluorescent probes for fluorescence sensors significantly affects sensor performance. CDs, with attributes such as large specific surface area, good electrical conductivity, biocompatibility, low toxicity, and high photostability, are promising candidates for sensor applications. This study focused on the application of CDs in dopamine detection across electrochemical, fluorescent, and

colorimetric sensors, and elucidates their construction processes and sensing mechanisms.

Several challenges persist in current CDs-based dopamine sensor research. (1) Despite synthesizing various CDs from diverse carbon source precursors, a comprehensive understanding of the CDs synthesis mechanism remains elusive, presenting a significant challenge. (2) Dopamine detection mechanisms using CDs from different synthesis methods vary, necessitating further investigation. (3) Although CDs-based sensors demonstrate advantages in dopamine detection, challenges such as the amalgamation of costly nanomaterials with CDs, intricate detection methods, inadequate storage stability, and potential nanoscale-associated concerns hinder their commercialization. It is suggested that these challenges can be addressed by ongoing CDs research, paving the way for mass-produced and widely applied CDs-based dopamine sensors in daily life.

Declaration of competing interest

The authors declare that they have no known competing financial interests or personal relationships that could have appeared to influence the work reported in this paper.

Acknowledgments

This work was supported by the National Natural Science Foundation of China (Nos. 82060599, 82360647), the Natural Science Foundation of Jiangxi Province (Nos. 20224BAB206091, 20232BAB216101), the Science and Technology Project of the Education Department of Jiangxi Province (No. GJJ2201406), the Natural Science Foundation of Ganzhou (No. 202101034482), the Science and Technology Project of Health Committee in Jiangxi Province (No. 202131033). At the same time, we are also very grateful to the precious advices raised by the editor and reviewers.

Supplementary materials

Supplementary material associated with this article can be found, in the online version, at doi:10.1016/j.cclet.2024.109598.

References

[1] G.A. Matthews, E.H. Nieh, C.M. Vander Weele, et al., Cell 164 (2016) 617–631.
[2] X. Li, S. Zhao, B. Li, et al., Coord. Chem. Rev. 431 (2021) 213686.
[3] A.J. Duszkiewicz, C.G. McNamara, T. Takeuchi, et al., Trends Neurosci. 42 (2019) 102–114.
[4] C. Bucolo, G.M. Leggio, F. Drago, et al., Pharmacol. Ther. 203 (2019) 107392.
[5] Y. Tang, J. Xu, C. Xiong, et al., Analyst 144 (2019) 2643–2648.
[6] R.P. Maas, T. Wassenberg, J.P. Lin, et al., Neurology 88 (2017) 1865–1871.
[7] Z. Tian, X. Qin, F. Shao, et al., Chin. Chem. Lett. 34 (2023) 107656.
[8] J. Li, A. Reimers, K.M. Dang, et al., Biosens. Bioelectron. 222 (2023) 114942.
[9] Q. Huang, S. Hu, H. Zhang, et al., Analyst 138 (2013) 5417–5423.
[10] Q. Huang, H. Zhang, S. Hu, et al., Biosens. Bioelectron. 52 (2014) 277–280.
[11] M.A. Elchisak, J.H. Carlson, Life Sci. 30 (1982) 2325–2336.
[12] J. Kim, M. Jeon, K.J. Paeng, et al., Anal. Chim. Acta 619 (2008) 87–93.
[13] Z. Chen, F. Zhang, Y. Lu, et al., Chin. Chem. Lett. 33 (2022) 3144–3150.
[14] X. Xu, R. Ray, Y. Gu, et al., J. Am. Chem. Soc. 126 (2004) 12736–12737.
[15] Y.P. Sun, B. Zhou, Y. Lin, et al., J. Am. Chem. Soc. 128 (2006) 7756–7757.
[16] W. Meng, B. Yang, S. Lu, Chin. J. Lumin. 42 (2021) 1075–1094.
[17] N. Dhull, G. Kaur, P. Jain, et al., Appl. Surf. Sci. 495 (2019) 143548.
[18] Z. Zeng, F.X. Xiao, H. Phan, et al., J. Mater. Chem. A 6 (2018) 1700–1713.
[19] Y. Wang, J. Sheng, X. Zhao, et al., Chin. Chem. Lett. 34 (2023) 107967.
[20] Y. Zhang, Q. Xie, Z. Xia, et al., J. Electroanal. Chem. 863 (2020) 114058.
[21] Q. Zeng, T. Feng, S. Tao, et al., Light: Sci. Appl. 10 (2021) 142.
[22] C. Xia, S. Zhu, T. Feng, et al., Adv. Sci. 6 (2019) 1901316.
[23] S. Zhang, Y. Yang, Y. Zhai, et al., Chin. Chem. Lett. 34 (2023) 107652.
[24] B. Wang, H. Wang, Y. Hu, et al., Nano Lett. 23 (2023) 8794–8800.
[25] P. Gao, Z. Xie, M. Zheng, Chin. Chem. Lett. 33 (2022) 1659–1672.
[26] X. Niu, W. Zheng, T. Song, et al., Chin. Chem. Lett. 34 (2023) 107560.
[27] X. Yang, X. Li, B. Wang, et al., Chin. Chem. Lett. 33 (2022) 613–625.
[28] B. Wang, S. Lu, Matter 5 (2022) 110–149.
[29] Y. Zhang, S. Lu, Chem 10 (2024) 134–171.
[30] Z. Wei, B. Wang, M. Xie, et al., Chin. Chem. Lett. 33 (2022) 751–756.
[31] Y. Zhang, J. Wang, L. Wang, et al., Adv. Mater. 35 (2023) 2302536.
[32] B. Wang, G.I.N. Waterhouse, S. Lu, Trends Chem. 5 (2023) 76–87.
[33] Y. Zhang, L. Wang, Y. Hu, et al., Small 19 (2023) 2207983.
[34] S. Wang, Y. Zhang, G. Pang, et al., Anal. Chem. 89 (2017) 1704–1709.
[35] L. Ding, S. Kang, Y. Wang, et al., Chin. J. Lumin. 44 (2023) 2002–2010.
[36] J. Du, N. Xu, J. Fan, et al., Small 15 (2019) e1805087.
[37] B. Wang, H. Cai, G.I.N. Waterhouse, et al., Small Sci. 2 (2022) 2200012.
[38] Y. Zhang, M. Li, S. Lu, Small 19 (2023) 2206080.
[39] M. Fang, B. Wang, X. Qu, et al., Chin. Chem. Lett. 35 (2024) 108423.
[40] B. Wang, H. Song, Z. Tang, et al., Nano Res. 15 (2022) 942–949.
[41] C. Liu, R. Cheng, J. Guo, et al., Chin. Chem. Lett. 33 (2022) 304–307.
[42] Y. Zhai, P. Wang, X. Zhang, et al., Chin. Chem. Lett. 33 (2022) 783–787.
[43] W. Zhao, Y. Wang, K. Liu, et al., Chin. Chem. Lett. 33 (2022) 798–802.
[44] G. Zou, S. Chen, N. Liu, et al., Chin. Chem. Lett. 33 (2022) 778–782.
[45] X. Li, X. Xing, S. Zhao, et al., Chin. Chem. Lett. 33 (2022) 1632–1636.
[46] X. Zhou, X. Wang, L. Shang, Chin. Chem. Lett. 34 (2023) 108093.
[47] N. Ahmed, W. Zareen, Y. Ye, et al., Chin. Chem. Lett. 33 (2022) 2765–2772.
[48] Q. Zhou, S. Wang, X. Ran, et al., Chin. Chem. Lett. 34 (2023) 107922.
[49] S. Zhuo, Y. Guan, H. Li, et al., Analyst 144 (2019) 656–662.
[50] X. Yang, F. Tian, S. Wen, et al., Processes 9 (2021) 170.
[51] M. Lakshmanakumar, N. Nesakumar, A.J. Kulandaisamy, et al., Measurement 183 (2021) 109873.
[52] L. Zhao, J. Liu, Y. Bai, et al., Colloids Surf. A. 627 (2021) 127179.
[53] M. Lan, S. Zhao, X. Wei, et al., Dyes Pigments 170 (2019) 107574.
[54] D.M. Liu, C. Dong, Process Biochem. 92 (2020) 464–475.
[55] Y.K. Cen, Y.X. Liu, Y.P. Xue, et al., Adv. Synth. Catal. 361 (2019) 5500–5515.
[56] S. Patra, S. Sene, C. Mousty, et al., ACS Appl. Mater. Interfaces 8 (2016) 20012–20022.
[57] Z. Tang, K. Jiang, S. Sun, et al., Analyst 144 (2019) 468–473.
[58] K.J. Mintz, Y. Zhou, R.M. Leblanc, Nanoscale 11 (2019) 4634–4652.
[59] S. Miao, K. Liang, J. Zhu, et al., Nano Today 33 (2020) 100879.
[60] S. Sun, Q. Guan, Y. Liu, et al., Chin. Chem. Lett. 30 (2019) 1051–1054.
[61] P. Krishnaiah, R. Atchudan, S. Perumal, et al., Chemosphere 286 (2022) 131764.
[62] J. Guo, W. Lu, H. Zhang, et al., Sens. Actuator. B: Chem. 330 (2021) 129360.
[63] L. Jiang, H. Ding, S. Lu, et al., Angew. Chem. Int. Ed. 59 (2020) 9986–9991.
[64] M. He, J. Zhang, H. Wang, et al., Nanoscale Res. Lett. 13 (2018) 175.
[65] M.E. Mahmoud, N.A. Fekry, A.M. Abdelfattah, J. Hazard. Mater. 397 (2020) 122770.
[66] F. Yang, W. Bao, T. Liu, B. Zhang, et al., Microchim. Acta 187 (2020) 322.
[67] J. Wang, X. Hu, H. Ding, et al., ACS Appl. Mater. Interfaces 11 (2019) 18203–18212.
[68] C. Wang, H. Shi, M. Yang, et al., J. Photochem. Photobiol. A 391 (2020) 112374.
[69] Y. Ma, A.Y. Chen, X.F. Xie, et al., Talanta 196 (2019) 563–571.
[70] C. Wang, H. Shi, M. Yang, et al., Colloids Surf. B 205 (2021) 111874.
[71] D. Mathivanan, A. Mohan, Y. Yang, J. Mater. Sci.: Mater. Electron. 32 (2021) 9005–9017.
[72] Q. Zhu, H. Mao, J. Li, et al., Spectrochim. Acta Part A 247 (2021) 119090.
[73] H. Liu, Y. Sun, Z. Li, et al., Nanoscale 11 (2019) 8458–8463.
[74] A.M. Mahmoud, M.H. Mahnashi, K. Alhazzani, et al., Spectrochim. Acta Part A 252 (2021) 119516.
[75] T. Zhao, J. Han, X. Jin, et al., Angew. Chem. Int. Ed. 58 (2019) 4978–4982.
[76] L.D. Rosales-Vazquez, A. Dorazco-Gonzalez, V. Sanchez-Mendieta, Dalton Trans. 50 (2021) 4470–4485.
[77] W.P. Lustig, S. Mukherjee, N.D. Rudd, et al., Chem. Soc. Rev. 46 (2017) 3242–3285.
[78] L. Li, Z. Li, W. Yang, et al., Chem 7 (2021) 686–698.
[79] X.X. Chen, M.J. Hou, G.J. Mao, Microchim. Acta 188 (2021) 287.
[80] D.X. Xue, Q. Wang, J. Bai, Coord. Chem. Rev. 378 (2019) 2–16.
[81] S. Xie, X. Li, L. Wang, et al., Microchem. J. 160 (2021) 105718.
[82] Y. Zhang, H. Xu, Y. Yang, et al., J. Photochem. Photobiol. A 411 (2021) 113195.
[83] Q. Yang, J. Li, X. Wang, et al., Sens. Actuator. B: Chem. 284 (2019) 428–436.
[84] M. Sun, L. Zhang, S. Xu, et al., Analyst 147 (2022) 947–955.
[85] C. Zhao, Y. Jiao, J. Hua, et al., J. Fluoresc. 28 (2018) 269–276.
[86] L. Wang, J. Jana, J.S. Chung, et al., Dyes Pigments 186 (2021) 109028.
[87] X.Y. Tang, Y.M. Liu, X.L. Bai, et al., Anal. Chim. Acta 1157 (2021) 338394.
[88] S.K. Tammina, D. Yang, S. Koppala, et al., J. Photochem. Photobiol. B 194 (2019) 61–70.
[89] R. Sangubotla, J. Kim, Dyes Pigments 191 (2021) 109364.
[90] R. Sangubotla, J. Kim, Mater. Sci. Eng. C 122 (2021) 111916.
[91] L. Ren, X. Hang, Z. Qin, et al., Optik 208 (2020) 163560.
[92] C. Ratlam, S. Phanichphant, S. Sriwichai, J. Polym. Res. 27 (2020) 183.
[93] S.W. Park, T.E. Kim, Y.K. Jung, Anal. Chim. Acta 1165 (2021) 338513.
[94] G. Mi, M. Yang, C. Wang, et al., Spectrochim. Acta Part A 253 (2021) 119555.
[95] M. Louleb, L. Latrous, Á. Ríos, et al., ACS Appl. Nano Mater. 3 (2020) 8004–8011.
[96] H. Lin, J. Huang, L. Ding, J. Nanomater. 2019 (2019) 5037243.
[97] A. Kumar, S. Asu, P. Mukherjee, et al., J. Photochem. Photobiol. A 406 (2021) 113019.
[98] J. Jana, J.S. Chung, S.H. Hur, ACS Omega 4 (2019) 17031–17038.
[99] S. Dadkhah, A. Mehdinia, A. Jabbari, et al., Microchim. Acta 187 (2020) 569.
[100] N. Chavoshi, B. Hemmateenejad, J. Fluoresc. 31 (2021) 455–463.
[101] J. Bai, X. Chen, G. Yuan, et al., Nano 16 (2021) 2150030.
[102] J. An, M. Chen, N. Hu, et al., Spectrochim. Acta Part A 243 (2020) 118804.
[103] A.O. Alqarni, S.A. Alkahtani, A.M. Mahmoud, et al., Spectrochim. Acta Part A 248 (2021) 119180.
[104] X. Tan, P. Zhang, C. Ye, et al., Dyes Pigments 180 (2020) 108515.

[105] R. Das, K.K. Paul, P.K. Giri, Appl. Surf. Sci. 490 (2019) 318–330.
[106] J. Wang, R. Du, W. Liu, et al., Sens. Actuator. B: Chem. 290 (2019) 125–132.
[107] G. Chellasamy, S.R. Ankireddy, K.N. Lee, et al., Mater. Today Bio 12 (2021) 100168.
[108] Q. Bai, H. Luo, X. Yi, et al., Microchem. J. 179 (2022) 107521.
[109] R. Zhang, Z. Fan, J. Photochem. Photobiol. A 392 (2020) 112438.
[110] Y. Liu, W. Li, P. Wu, et al., Sens. Actuator. B: Chem. 281 (2019) 34–43.
[111] K. Chaiendoo, S. Ittisanronnachai, V. Promarak, et al., Carbon 146 (2019) 728–735.
[112] S. Wei, B. Liu, X. Shi, et al., Talanta 252 (2023) 123865.
[113] R. Sangubotla, J. Kim, Ceram. Int. 49 (2023) 16272–16282.
[114] X. Liu, W. Yu, X. Mu, et al., Spectrochim. Acta Part A 287 (2023) 122112.
[115] A. Tiwari, S. Walia, S. Sharma, et al., J. Mater. Chem. B 11 (2023) 1029–1043.
[116] W. Guo, Q. Wang, X. Zhan, et al., Part. Part. Syst. Charact. 39 (2022) 2200089.
[117] S. Kanagasubbulakshmi, K. Kadirvelu, Spectrochim. Acta Part A 206 (2019) 512–519.
[118] W. Liu, X.J.T. Zhu, Talanta 197 (2019) 59–67.
[119] H. Liu, N. Li, H. Zhang, et al., Talanta 189 (2018) 190–195.
[120] Y. Guo, S. Guo, Y. Fang, et al., Electrochim. Acta 55 (2010) 3927–3931.
[121] Y. Mei, C. He, W. Zeng, et al., Food Bioprocess Technol. 15 (2022) 498–513.
[122] Y. Sun, M. Luo, X. Meng, et al., Anal. Chem. 89 (2017) 3761–3767.
[123] H. Zhang, K.-T. Huang, L. Ding, et al., Chin. Chem. Lett. 33 (2022) 1537–1540.
[124] Y. Yu, M. Pan, J. Peng, et al., Chin. Chem. Lett. 33 (2022) 4133–4145.
[125] H. Liu, Y. Yu, T. Xue, et al., Chin. Chem. Lett. 35 (2024) 108574.
[126] X. Lin, Y. Mei, C. He, et al., Front. Chem. 9 (2021) 769648.
[127] Y. Jiang, X. Xiao, C. Li, et al., Anal. Chem. 92 (2020) 3981–3989.
[128] H. Wei, F. Wu, L. Li, et al., Anal. Chem. 92 (2020) 11374–11379.
[129] A. Joshi, W. Schuhmann, T.C. Nagaiah, Sens. Actuator. B: Chem. 230 (2016) 544–555.
[130] Y. Wu, P. Deng, Y. Tian, et al., J. Nanobiotechnol. 18 (2020) 112.
[131] Q. Huang, X. Lin, D. Chen, et al., Food Chem. 373 (2022) 131415.
[132] Z. Wang, Int. J. Electrochem. Sci. 16 (2021) 210450.
[133] L. Li, Y. Chen, J.J. Zhu, Anal. Chem. 89 (2017) 358–371.
[134] J. Zhou, Y. Li, W. Wang, et al., Biosens. Bioelectron. 164 (2020) 112332.
[135] J. Liu, Y. Zhang, R. Yuan, Sens. Actuator. B: Chem. 379 (2023) 133260.
[136] Z. Zhu, H. Niu, R. Li, et al., Biosens. Bioelectron. 10 (2022) 100141.
[137] F. Xie, M. Yang, M. Jiang, et al., TrAC Trends Anal. Chem. 119 (2019) 115624.
[138] A. Chen, S. Chatterjee, Chem. Soc. Rev. 42 (2013) 5425–5438.
[139] B.R. Adhikari, M. Govindhan, A. Chen, Sensors 15 (2015) 22490–22508.
[140] Q. Huang, X. Lin, L. Tong, et al., ACS Sustain. Chem. Eng. 8 (2020) 1644–1650.
[141] Q. Pan, Z. Xu, S. Deng, et al., RSC Adv. 9 (2019) 39332–39337.
[142] Y.Y. Li, P. Kang, S.Q. Wang, et al., Sens. Actuator. B: Chem. 327 (2021) 128878.
[143] G. Han, J. Cai, C. Liu, J. Ren, et al., Appl. Surf. Sci. 541 (2021) 148566.
[144] E. Saeb, K. Asadpour-Zeynali, Microchem. J. 160 (2021) 105603.
[145] M. Mehmandoust, P. Pourhakkak, F. Hasannia, et al., Food Chem. Toxicol. 164 (2022) 113080.
[146] N. Ahmadi, M. Bagherzadeh, A. Nemati, Biosens. Bioelectron. 151 (2020) 111977.
[147] J.M. Moon, N. Thapliyal, K.K. Hussain, et al., Biosens. Bioelectron. 102 (2018) 540–552.
[148] S. Samanta, P. Roy, P. Kar, Mater. Sci. Eng. B 256 (2020) 114541.
[149] A. John, L. Benny, A.R. Cherian, et al., J. Nanostruct. Chem. 11 (2021) 1–31.
[150] Y. Wang, A. Liu, Y. Han, et al., Polym. Int. 69 (2019) 7–17.
[151] M.Z. Iqbal, M.M. Faisal, S.R. Ali, et al., Electrochim. Acta 346 (2020) 136039.
[152] Q. Wang, J. Li, D. Wang, et al., Electrochim. Acta 349 (2020) 136348.
[153] Y. Prykhodko, K. Fatyeyeva, L. Hespel, et al., Chem. Eng. J. 409 (2021) 127329.
[154] P. Senthil Kumar, B.S. Sreeja, K. Krishna Kumar, et al., Food Chem. Toxicol. 167 (2022) 113311.
[155] H.S. Jang, D. Kim, C. Lee, et al., Inorg. Chem. Commun. 105 (2019) 174–181.
[156] L. Yang, T. Wang, C. Bao, et al., J. Electroanal. Chem. 895 (2021) 115512.
[157] B. Wu, M. Li, Z. Xu, et al., Simultaneous electrochemical detection of dopamine and uric acid with graphene quantum dots decorated cobalt phthalocyanine nanocomposite, in: 21st International Conference on Solid-State Sensors, Actuators and Microsystems (Transducers), IEEE, 2021, pp. 533–536, doi:10.1109/Transducers50396.2021.9495550.
[158] Y. Wei, Z. Xu, S. Wang, et al., Ionics 26 (2020) 5817–5828.
[159] J. Wang, C. Lu, T. Chen, et al., Nanophotonics 9 (2020) 3831–3839.
[160] V. Vinoth, L.N. Natarajan, R.V. Mangalaraja, et al., Microchim. Acta 186 (2019) 681.
[161] P. Thondaiman, R. Manikandan, C.J. Raj, et al., Synth. Met. 278 (2021) 116831.
[162] S. Saisree, N.J.S. Arya, K.Y. Sandhya, J. Mater. Chem. B 10 (2022) 3974–3988.
[163] T.M. Prado, A. Carrico, F.H. Cincotto, et al., Sens. Actuator. B: Chem. 285 (2019) 248–253.
[164] P.K. Pandey, Preeti, K. Rawat, T. Prasad, et al., J. Mater. Chem. B 8 (2020) 1277–1289.
[165] N. Ndebele, P. Sen, T. Nyokong, J. Electroanal. Chem. 886 (2021) 115111.
[166] M. Li, Int. J. Electrochem. Sci. 16 (2021) 21084.
[167] K. Kunpatee, S. Traipop, O. Chailapakul, et al., Sens. Actuator. B: Chem. 314 (2020) 128059.
[168] W.F. Hsu, T.M. Wu, J. Mater. Sci. 30 (2019) 8449–8456.
[169] S.E. Elugoke, O.E. Fayemi, A.S. Adekunle, et al., FlatChem 33 (2022) 100372.
[170] S.K. Arumugasamy, S. Govindaraju, K. Yun, Appl. Surf. Sci. 508 (2020) 145294.
[171] G. Huang, X. Yang, R. Huang, Int. J. Electrochem. Sci. 15 (2020) 9888–9901.
[172] C. Luhana, I. Moyo, K. Tshenkeng, et al., Microchem. J. 180 (2022) 107605.
[173] T. Zhang, D. Long, X. Gu, et al., Microchim. Acta 189 (2022) 389.
[174] R. Wu, S. Yu, S. Chen, et al., Anal. Chim. Acta 1229 (2022) 340365.
[175] J. Zhou, Y. Xia, Z. Zou, et al., Anal. Chim. Acta 1237 (2023) 340631.
[176] F. Nosratzehi, H. Halakoei, M. Rostami, et al., Diamond Relat. Mater. 127 (2022) 109120.
[177] A. Thadathil, D. Thacharakkal, Y.A. Ismail, et al., Biosensors 12 (2022) 1063.
[178] H. Chul Lim, S.J. Jang, Y. Cho, et al., ChemElectroChem 9 (2022) e202200557.
[179] Z. Nazari, M. Hadi Nematollahi, F. Zareh, et al., ChemistrySelect 8 (2023) e202203630.
[180] K. Wang, Y. Li, M. Qi, et al., Microchim. Acta 189 (2022) 382.
[181] M. Hasheena, A. Ratnamala, M. Noorjahan, et al., J. Appl. Electrochem. 53 (2022) 571–583.
[182] J.H.A. Ferreira, R.M. Peres, M. Nakamura, et al., J. Nanopart. Res. 25 (2023) 9.
[183] B. Liu, J. Zhuang, G. Wei, Environ. Sci. 7 (2020) 2195–2213.
[184] S. He, Q. Huang, Y. Zhang, et al., Chin. Chem. Lett. 32 (2021) 1462–1465.
[185] Y. Chen, X. Yang, C. Lu, et al., Chin. Chem. Lett. 34 (2023) 108099.
[186] Y.T. Huang, M. Xue, Y. Yang, Chin. Chem. Lett. 34 (2023) 108294.
[187] Z. Jia, Y. Liu, L. Cheng, et al., Talanta 11 (2023) 1288418.
[188] T. Alawsi, G.P. Mattia, Z. Al-Bawi, et al., Sens. Bio-Sensing Res. 32 (2021) 100404.
[189] C. Dong, X. Ma, N. Qiu, et al., Sens. Actuator. B: Chem. 329 (2021) 129066.
[190] Monisha, K. Shrivas, T. Kant, et al., J. Hazard. Mater. 414 (2021) 125440.
[191] R. Wang, G. Ruan, Y. Sun, et al., Dyes Pigments 191 (2021) 109383.
[192] Y. Zhang, Q. Luo, K. Ding, et al., Sens. Actuator. B: Chem. 335 (2021) 129708.
[193] W. Liu, Z. Li, H. Jia, et al., Appl. Surf. Sci. 481 (2019) 678–683.
[194] H. Singh, A. Bamrah, S.K. Bhardwaj, et al., Environ. Sci. 8 (2021) 863–889.
[195] R. Singh, R. Mehra, A. Walia, et al., Int. J. Environ. Anal. Chem. 103 (2023) 1361–1376.
[196] M. Amiri, S. Dadfarnia, A.M. Haji Shabani, et al., J. Pharm. Biomed. Anal. 172 (2019) 223–229.
[197] Y.F. Wang, L. Li, M. Jiang, et al., Appl. Surf. Sci. 573 (2022) 151457.
[198] Y. Xu, J. Wang, Y. Lu, et al., Spectrochim. Acta Part A 219 (2019) 225–231.
[199] V. Naik, P. Zantye, D. Gunjal, et al., ACS Appl. Bio Mater. 2 (2019) 2069–2077.